Eur. Phys. J. B **10**, 641–648 (1999)

THE EUROPEAN PHYSICAL JOURNAL B

EDP Sciences

Influence of atomic order on $TA_1[110]$ phonon softening and displacive phase transition in $Fe_{72}Pt_{28}$ Invar alloys

J. Kästner[1,a], W. Petry[2], S.M. Shapiro[3], A. Zheludev[3], J. Neuhaus[2], Th. Roessel[1], E.F. Wassermann[1], and H. Bach[4]

[1] Labor für Tieftemperaturphysik and SFB 166, Gerhard-Mercator-Universität Duisburg, 47048 Duisburg, Germany
[2] Physik Department E13, Technische Universität München, 85747 Garching, Germany
[3] Brookhaven National Laboratory, Upton, New York 11973, USA
[4] Institut für Experimentalphysik IV and SFB 166, Ruhr Universität Bochum, 44780 Bochum, Germany

Received 18 January 1999

Abstract. The acoustic phonon dispersions of two Invar crystals $Fe_{72}Pt_{28}$, one ordered with the $L1_2$ (Cu_3Au) structure, the other disordered fcc, have been investigated between 3.4 K and 470 K by inelastic and elastic neutron scattering. For the ordered crystal, pronounced softening of the whole $TA_1[\xi\xi 0]$ phonon branch is observed on cooling below the Curie temperature. Particularly strong phonon softening at the M-point zone boundary of the $L1_2$ structure leads to a displacive, antiferrodistortive phase transition at low temperatures. For the disordered crystal, much weaker softening of the $TA_1[\xi\xi 0]$ phonons is observed and restricted to the region near the Brillouin zone center, where increasing elastic scattering with decreasing temperature indicates the growth of local tetragonal strain. This strain is considered as a typical precursor of the transformation to bct martensite. Specific heat measurements, performed at low temperatures on both crystals confirm the neutron scattering results and reveal considerable enhancement of the low energy phonon density of states in the ordered crystal.

PACS. 63.20.Dj Phonon states and bands, normal modes, and phonon dispersion – 64.70.Kb Solid-solid transitions – 65.40.+g Heat capacities of solids

1 Introduction

The magnetic and structural properties of the fcc Fe-rich transition metal alloys have been the subject of continuous interest in physics and metallurgy. Recent intensive experimental and theoretical investigations of the magnetovolume properties, namely of the Invar effect and the related phenomena in these alloys [1,2] have provided a quite detailed microscopic picture of the nature of 3d-magnetism and of its influence on the structural stability of the fcc Fe-rich alloys and of the fcc element Fe itself [3–5].

It is now well understood that the fcc 3d-alloys containing Fe or Mn exhibit an instability of the magnetic moment with respect to changes in the atomic electron concentration and the volume. This instability is reflected in the Invar effect; a small or even negative thermal expansion below the magnetic ordering temperatures of the alloys due to thermal fluctuations from a high-volume high-moment ground state to low energy excited states with low volume and low magnetic moment. In the fcc alloys with composition close to pure Fe the anti-Invar effect is observed; an enhanced thermal expansion at high temperatures in the paramagnetic range due to thermal fluctuations from a low-volume low-magnetic-moment ground state to excited states with high volume and high magnetic moment [5,6].

With increasing Fe-content and decreasing temperature, the alloys undergo a martensitic phase transformation from the high temperature fcc austenite (γ-Fe) into the bcc martensite (α-Fe). Recent theoretical investigations based on first principle calculations of the martensitic phase transition in Fe-Ni Invar [3,7] suggest that the instability of the fcc lattice is essentially related to the instability of the Fe-magnetic moment which depends on the mean valence electron concentration, the atomic volume and the local environment of the Fe atoms.

Considering the lattice dynamics of the martensitic transformation, we know that many early transition metals, transforming from the high temperature open bcc to the low temperature closed packed hcp structure, exhibit considerable softening of transverse acoustic phonons in the high temperature phase on approach of M_S, the transformation start temperature [8]. In the closed packed fcc Invar alloys Fe-Ni, Fe-Pd, and Fe-Pt, which transform into the more open bcc or bct martensite at low temperatures, phonon softening preceding the martensitic transition appears less clear. Ultrasonic [9] and neutron scattering [10–12] results reveal, however, significant softening of the shear related to the elastic constant C' and the long wavelength $TA_1[\xi\xi 0]$ phonons,

[a] e-mail: kaestner@ttphysik.uni-duisburg.de

i.e. with polarization along $[1\bar{1}0]$ in these alloys below their Curie temperatures. Besides this long wave length shear, the idea of phonon softening in the Invar alloys as being a precursor to the martensitic transformation is not well established.

The Fe-Pt alloys of composition near Fe_3Pt, for which the Invar effect is large and the martensitic transition appears at low temperatures, exhibit the unique property that they can be investigated either in the disordered fcc or in the ordered Cu_3Au ($L1_2$) structure with different degrees of atomic order. Their magnetic, magnetovolume and thermal properties as well as the concentration dependence of the structural phase boundaries strongly depend on the degree of atomic order [13–15]. Neutron scattering experiments, so far performed only on ordered Fe-Pt Invar alloys [10,16], demonstrate that softening of the $TA_1[\xi\xi 0]$ phonons exists throughout the Brillouin zone, but is particularly strong at the M-point zone boundary [16].

In this report (paper I) we present results of neutron scattering experiments on two $Fe_{72}Pt_{28}$ crystals, one ordered in the $L1_2$ structure, the other disordered fcc. Both crystals are close to but stable with respect to the occurence of the martensitic phase down to zero Kelvin. Our interest is focused on the lattice dynamics and the related structural changes in both samples within the premartensitic region, as well as on the low temperature thermal excitations depending on the degree of atomic order. In another article (paper II) we report on neutron scattering results obtained for two ordered Fe-Pt crystals with compositions even closer to and right at the martensitic phase boundary. In that paper, our interest is focused on the behaviour of the $TA_1[\xi\xi 0]$ phonon softening with approach to and crossing of the martensitic phase boundary. The results are discussed in relation to the structural changes observed during the martensitic transformation. A low temperature structural phase diagram of ordered Fe-Pt alloys with compositions near Fe_3Pt will be presented.

2 Experiment

The $Fe_{72}Pt_{28}$ crystals were prepared using a Stockbarger-Bridgman method. Appropriate amounts of 99.98% pure Fe and 99.95% pure Pt were molten in Al_2O_3 crucibles by inductive heating under Argon atmosphere. Single crystals of 2 to 3 cm length and 1 cm diameter were grown with solidification rate of 1 mm/h. Initial annealing and homogenization at about 1 300 K for several hours was followed by checking the single crystallinity with X-rays at the sample surface at room temperature using the Laue method. The disordered fcc or the ordered structure $L1_2$ was achieved by re-heating the crystals to well above the ordering temperature $T_0 \approx 750\,^{\circ}\mathrm{C}$ and then either subsequent quenching to room temperature (disordered state) or annealing 1 hr at 800 °C, 1 day at 700 °C, 3 days at 600 °C, 10 days at 500 °C, and 30 days at 450 °C (ordered state). As determined by X-ray diffraction on many polycrystalline samples of similar composition, this thermal treatment results in long range order parameters $S \leq 0.2$ for disordered crystals and $0.90 \leq S \leq 0.95$ for ordered crystals with Pt-content between 25 and 28 at%.

Composition and homogeneity of the investigated crystals were checked by energy dispersive X-ray analysis which gave results that agree with the nominal value within ±1 at%. Taking rocking curves through the (200) reflection with neutrons gave mosaic spreads of 0.4° (fwhm) for the ordered and disordered crystal.

Elastic and inelastic neutron scattering were performed with the three-axis spectrometers H4M and H7 at the Brookhaven reactor. Pyrolitic graphite crystals were used as monochromator and analyser. A graphite filter was used to suppress higher order contamination of the constant final wave vector $k_f = 2.67$ Å^{-1} before the analyser. Typical collimation of 40′-20′-20′-40′ was used.

Several acoustic phonon dispersions of the two crystals were determined at different temperatures along high symmetry directions. The $TA_1[\xi\xi 0]$ phonon branch was determined in more detail mainly by taking constant q-scans at various temperatures between 470 K and 3.4 K within the (001) scattering plane between the (200) and $(3\bar{1}0)$ as well as between the (220) and (310) Bragg reflections. The $TA_1[\xi\xi 0]$ phonon energies $\hbar\omega_0$ and damping constants Γ_0 were determined by fitting damped oscillator functions to the observed intensity spectra $I(\omega, T)$ convoluted by the resolution functions of the spectrometers.

3 Results and discussion

3.1 $TA_1[\xi\xi 0]$ phonon dispersion

Among the acoustic phonon modes investigated along the main symmetry directions, only the $TA_1[\xi\xi 0]$ phonons show considerable softening with decreasing temperature. As observed previously on all Fe-rich Invar alloys [10–12], this softening apparently starts near the Curie temperature, which is $T_C^o \approx 500$ K and $T_C^d \approx 375$ K for ordered and disordered $Fe_{72}Pt_{28}$, respectively. Here we report mainly on results of the $TA_1[\xi\xi 0]$ phonon dispersion behaviour at lower temperatures.

In Figure 1, the energy of the $TA_1[\xi\xi 0]$ branch determined at different temperatures for both crystals is plotted *vs.* the reduced wave vector ξ in units of $2\pi/a$ of the reciprocal fcc lattice. The figure shows that the disordered crystal exhibits considerable phonon softening in the inner region of the Brillouin zone ($\xi < 0.4$) on cooling to below room temperature. The ordered crystal shows similar behaviour in the low ξ-range but additionally exhibits a pronounced soft phonon mode around $\xi = 0.5$. This value corresponds to the M-point zone boundary of the simple cubic lattice, the base lattice of the $L1_2$ structure. Whereas the phonon dispersion of this crystal at 470 K, closely below $T_C^o \approx 500$ K, is weak, the phonon energies near and right at the zone boundary decrease rapidly on reduction of the temperature to small but not completely zero values.

For a closer inspection of the phonon softening in both crystals and for comparison with intensities of elastic

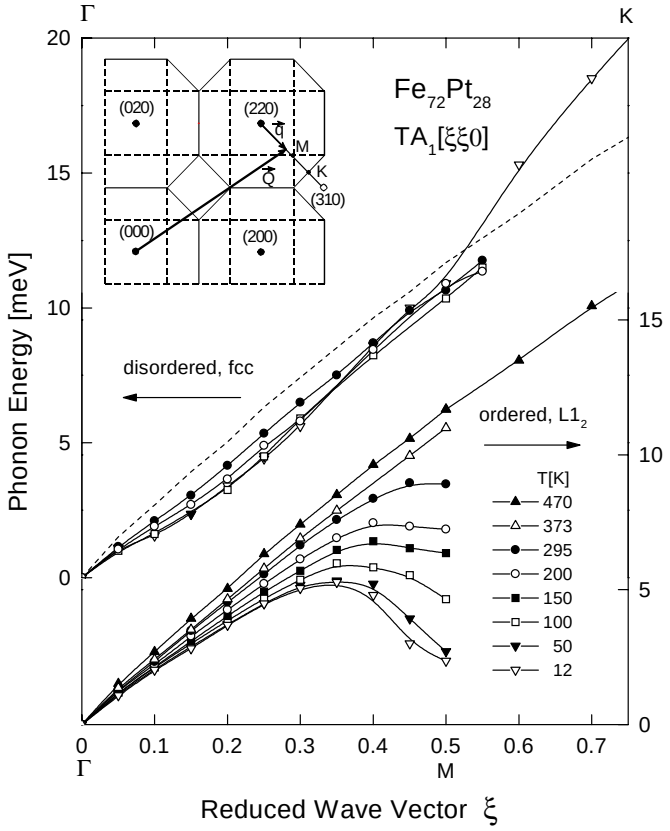

Fig. 1. $TA_1[\xi\xi 0]$ phonon energies for ordered and disordered $Fe_{72}Pt_{28}$ at different temperatures. Lines are guide to the eyes. Dashed line denotes phonon branch of ordered crystal at 470 K.

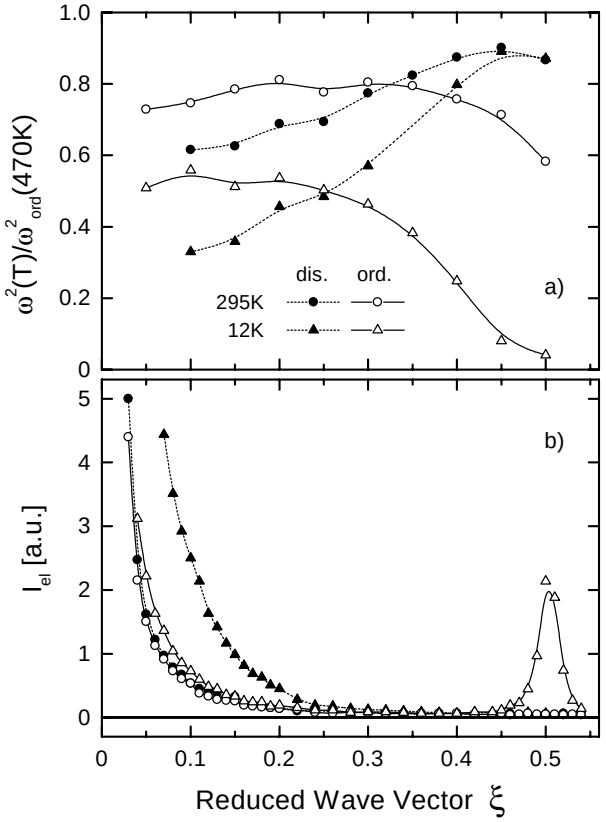

Fig. 2. (a) Squared $TA_1[\xi\xi 0]$ phonon frequencies normalized to ordered crystal at 470 K and (b) elastic scattering intensities *vs.* ξ for 295 K and 12 K. Open and solid symbols refer to ordered and disordered crystal, respectively. Lines are guide to the eyes.

scattering we have plotted the square of the phonon frequencies $\omega^2(\xi, T)$, normalized to $\omega^2_{\rm ord}(\xi, 470\ {\rm K})$ of the ordered crystal in Figure 2a for temperatures T = 12 K and 295 K. In Figure 2b, the corresponding elastic scattering intensities $I_{\rm el}(\xi, T)$ are shown for the same temperatures. Figure 2a suggests that for disordered $Fe_{72}Pt_{28}$ the phonon softening is most pronounced around $\xi = 0.1$ at low temperatures. A softening extending to even smaller ξ and right to the zone center, related to a decrease of the elastic constant C', as observed by ultrasonic measurements [9,17], cannot be inferred from the present data because of the limited resolution of the spectrometer. Furthermore, as can be seen already in Figure 1, the disordered crystal exhibits no phonon softening at all at the M-point. In the ordered crystal, on the contrary, the whole part of the $TA_1[\xi\xi 0]$ phonon branch above $\xi \approx 0.2$ is clearly dominated by the strong softening of the M-point zone boundary mode, whereas phonon softening within the inner part of the Brillouin zone is also present but apparently less than that of the disordered crystal. We note that absolute values may depend to some degree on the normalization of the phonon frequencies. The distinctly different softening behaviour of the transverse acoustic phonons in both crystals is, however, independent of the choice of normalization and thus a physical result related to the atomic ordering, *i.e.* to the local environment of the Fe- and Pt atoms.

The ξ-dependence of the elastic scattering intensities from both crystals, shown in Figure 2b, is quite complementary to the phonon softening behaviour, shown in Figure 2a. For disordered $Fe_{72}Pt_{28}$, strongly enhanced Huang like scattering at small ξ up to $\xi \approx 0.2$ appears on cooling to low temperatures. This suggests the development of local tetragonal shear strain distorting the fcc lattice cells, similar to what is observed *e.g.* in fcc $Fe_{70}Pd_{30}$ as precursor of the fcc-fct phase transition [18]. For ordered $Fe_{72}Pt_{28}$, however, the elastic scattering at small ξ is much less enhanced at low temperatures. Instead, a well defined superstructure peak develops at the M-point on the decrease of temperature. This zone boundary peak reveals the occurence of a displacive phase transition at low temperatures. The transition is "antiferrodistortive", *i.e.* the unit cell of the low temperature lattice is twice as large as that of the $L1_2$ structure — analogous to the "antiferromagnetic" transition, where the magnetic unit cell is doubled with respect to the atomic unit cell of the lattice.

Since neither the investigated fcc crystal is completely disordered nor the $L1_2$ crystal perfectly ordered, one may expect on the one hand that the soft M-mode should lower the phonon frequencies of the disordered crystal to some extent due to residual long range order. In the disordered

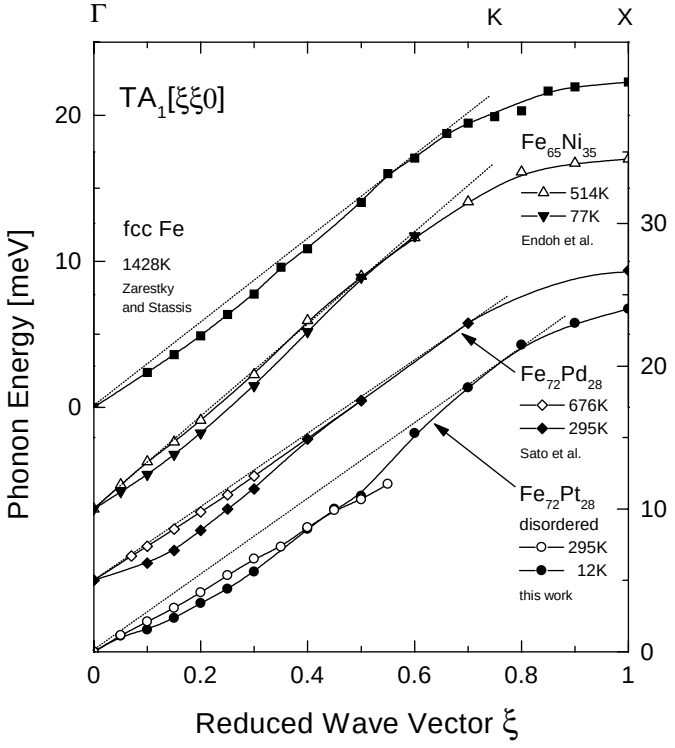

Fig. 3. $TA_1[\xi\xi 0]$ phonon energies *vs.* ξ for fcc $Fe_{72}Pt_{28}$, $Fe_{65}Ni_{35}$ [11], $Fe_{72}Pd_{28}$ [12], and Fe [19] at different temperatures. Lines are guide to the eyes. Dotted lines are shown to visualize the positive curvature of the phonon branches.

crystal, a slight temperature dependence of the phonon frequency near the M-point, as shown in Figure 1, is indeed observed. This frequency change is, however, not systematic with respect to the change of the temperature and lies almost within the error of the measurement. On the other hand one may expect that some structural disorder in the ordered crystal — *e.g.* due to non-stoichiometry, anti-site atoms and anti-phase boundaries — hinders the M-mode from softening to almost zero energy. Furtheron, magnetic disorder, *i.e.* magnetic domains are considered to influence the mode softening and damping in ordered $Fe_{72}Pt_{28}$ at low temperatures. This will be discussed further below in this article. In addition, we suspect that a mutual interaction between the long and short wave phonon frequencies and strains exists. This will be discussed within paper II.

In Figure 3, the $TA_1[\xi\xi 0]$ phonon branches for disordered fcc $Fe_{72}Pt_{28}$ and the Fe-rich fcc Invar alloys $Fe_{65}Ni_{35}$ [11], $Fe_{72}Pt_{28}$ [12], and for fcc Fe [19] at different temperatures are plotted for comparison. Common to all branches is a positive curvature in the range $0 < \xi < 0.6$, similar as found for the fcc noble metals. In addition, the three Fe-rich ferromagnetic (FM) alloys exhibit remarkable phonon softening in the range $\xi < 0.5$ on cooling below their Curie temperatures. This softening is attributed to the ξ-dependent electron-phonon interaction due to changes of the *d*-band electronic structure accompanied with long range magnetic ordering. Calculations of the phonon frequencies in Fe_3Ni [20] and Fe_3Pt [21], based on first principle electronic band structure calculations, confirm these considerations. They show that with the assumption of short range interatomic forces determining the overall phonon frequencies, the details such as ξ-dependent anomalies of the phonon branches are quite well described by long range force fields, depending on the electron-phonon scattering near the Fermi surface. From a quite different approach, based on the theory of elasticity, a positive curvature of the $TA_1[\xi\xi 0]$ phonon branch in the small ξ-range, *e.g.* of Fe-Pd, was derived from the existence of fct strain gradients within the material [22].

As mentioned above, the decrease of the long wave $TA_1[\xi\xi 0]$ phonon energies with the drop of temperature in disordered fcc $Fe_{72}Pt_{28}$ and in the other FM Fe-rich fcc alloys indicates that the fcc lattice becomes increasingly unstable against the long wave shear strain and may undergo the fcc-fct transition if the shear constant C' becomes sufficiently small. Actually, a weakly first order fcc-fct transformation was observed and studied in detail in some Fe-Pd alloys with compositions close to the bct martensite phase boundary [23–25]. Similarily, electron microscopy and X-ray investigations on fcc Fe-Pt alloys [24,26] have revealed the fct phase at low temperatures near the phase boundary to the bct martensite. This implies that a small C' constant and soft long wave $TA_1[\xi\xi 0]$ phonons may as well influence the kinetics of the martensitic transformation into the bct structure. From the orientation relations observed between the lattices of ferrous austenite and martensite it is deduced that the transformation is promoted mainly by long wave shear along the close packed fcc (111) planes, where a small shear constant C' in combination with C_{44} plays an essential role [27]. We shall discuss this aspect in further detail in paper II.

3.2 Zone boundary soft mode

For the discussion of the soft phonon mode behaviour at the M-point zone boundary in ordered $Fe_{72}Pt_{28}$, some of the phonon scattering intensities $I(\omega, T)$ determined at various fixed temperatures between 3.4 K and 100 K, are shown in Figure 4. Above about 50 K, the cross sections exhibit rather broad maxima, indicating that the zone boundary phonons are considerably damped even at high temperatures. Below 50 K, no maxima are observed at all and the phonon modes become overdamped. Note that significant scattering intensity measured up to energies $\sim$ 7 meV hardly changes with further decrease of the temperature. Simultaneously, a central component $I(\omega = 0, T)$ in the cross section rapidly develops. The ξ- and T-dependence of this scattering is shown in Figures 2 and 6a, respectively. The central component, the energy width of which is given by the resolution width of the spectrometer, is supposed to be of static nature. Taking into account this central component, the solid curves in Figure 4 represent fits to the experimental cross sections according to damped oscillator modes. The arrows mark the mode energies $\hbar\omega_0$ determined at the different temperatures, respectively.

Results of these fits and of those obtained at higher temperatures are collected in Figure 5. The inset

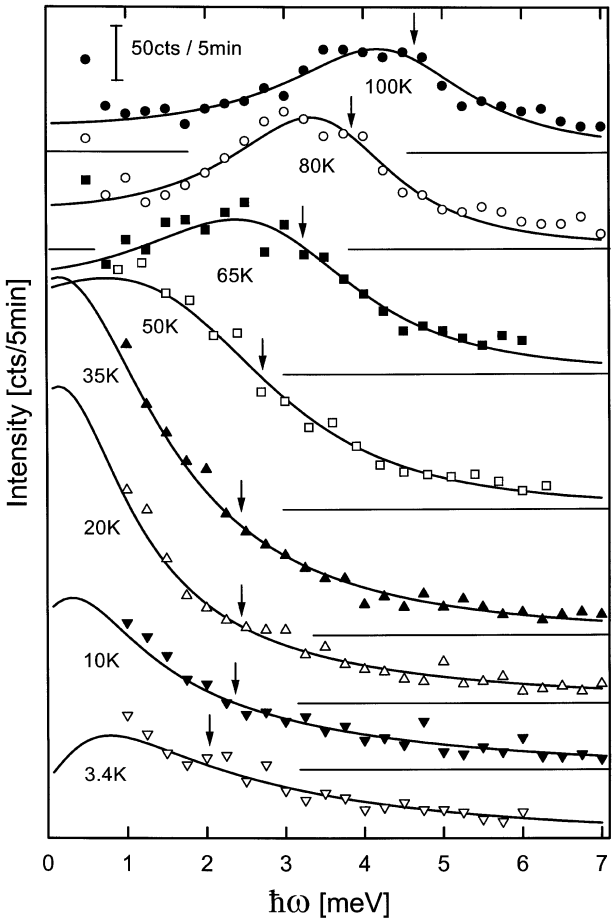

Fig. 4. $TA_1 0.5[110]$ phonon scattering cross sections for ordered $Fe_{72}Pt_{28}$ at different temperatures. Solid curves are fits according damped oscillator functions. Arrows mark the mode energies, respectively.

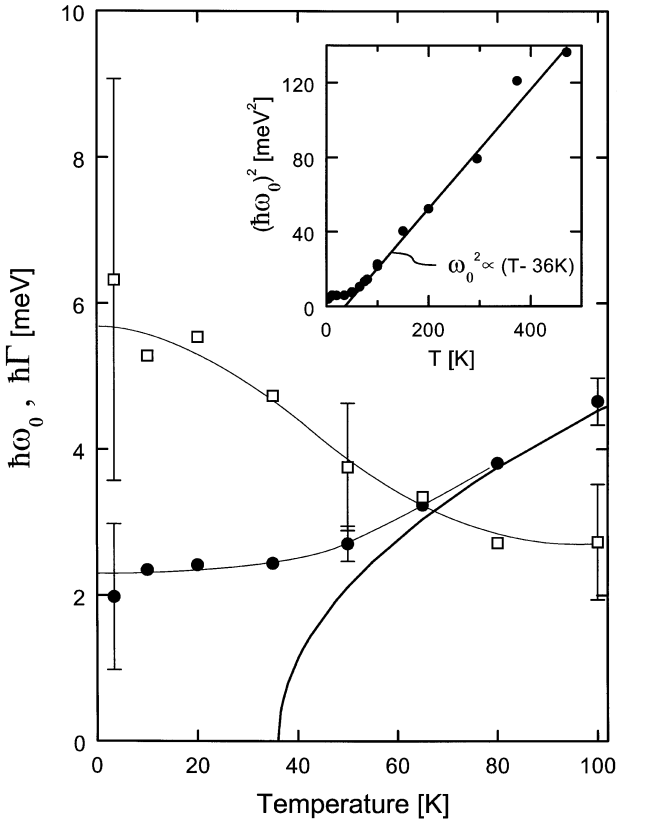

Fig. 5. Phonon energies $\hbar\omega_0$ (•) and damping constants $\hbar\Gamma$ (□) *vs.* temperature for $TA_1 0.5[110]$ mode in ordered $Fe_{72}Pt_{28}$. The inset shows the Curie-Weiss behaviour $\omega_0^2 \propto (T - 36\ \mathrm{K})$ (straight line and solid curve in the main figure, respectively). Thin lines are guides to the eyes.

of Figure 5 shows, that the inverse zone boundary mode susceptibility is well described by a Curie-Weiss law $\omega_0^2 \propto (T - T_1)$ between about 80 K and 300 K with a critical temperature $T_1 \approx 36$ K. Though this Curie-Weiss law seems to hold also above 300 K, its validity becomes questionable with approach to the magnetic Curie temperature $T_C \approx 500$ K. In the vicinity of T_C, one expects that the $TA_1[\xi\xi 0]$ phonon frequencies vary more strongly with T, *i.e.* like the elastic shear constant $C' \propto M^2(T)$, the square of the spontaneous magnetization [17,28], and that further above T_C they decrease again. As will be shown in paper II, the observed incipient softening of the $TA_1 0.5[110]$ zone boundary mode at high temperatures is, however, not sensitively dependent on the different Curie temperatures of the investigated Fe-Pt crystals.

Apart from such peculiar behaviour at high temperatures around T_C, Figure 5 shows that significant deviation from a Curie-Weiss behaviour of the phonon frequencies occurs below about 80 K. The quasi harmonic mode energy levels off to approach a temperature independent value $\hbar\omega_0 \approx 2.3$ meV. Simultaneously, the damping $\hbar\Gamma$ increases with the drop of temperature as the elastic scattering intensity does similarly (see Fig. 6a). We conclude that the increase of the elastic scattering and of the phonon damping at the M-point in ordered $Fe_{72}Pt_{28}$ arises from the displacive transition of the $L1_1$-structure into a premartensitic antiferrodistorted phase at low temperatures. This phase distinctly differs from the premartensitic locally ferrodistorted fct phase in disordered fcc $Fe_{72}Pt_{28}$. Our conclusions are corroborated by previous observations of low temperature anomalies in the thermal expansion [29,30], the high and low field magnetization [31,32] and the low field a.c. magnetic susceptibility [33] of ordered Fe-Pt alloys with composition close to Fe_3Pt.

Following the notation of Noda and Endoh, who determined the complete phonon spectrum of ordered $Fe_{73}Pt_{27}$ in the high symmetry directions and in particular the $TA_1 0.5[110]$ zone boundary phonon energies down to 80 K [16], we expect that the soft zone boundary mode in ordered Fe_3Pt is either the M_4- or the M_2-mode. These zone boundary modes are characterized by displacements of only the Fe-atoms within the $L1_2$-structure. For the M_4-mode, the Fe-atoms move within the (100)-cube faces, as indicated in the inset of Figure 6a. For the M_2-mode they move perpendicularly out of the (100) faces. Our assumption that the M_4-mode is the predominating soft mode is supported by recent theoretical results on the phonon softening due to the electron-phonon interaction

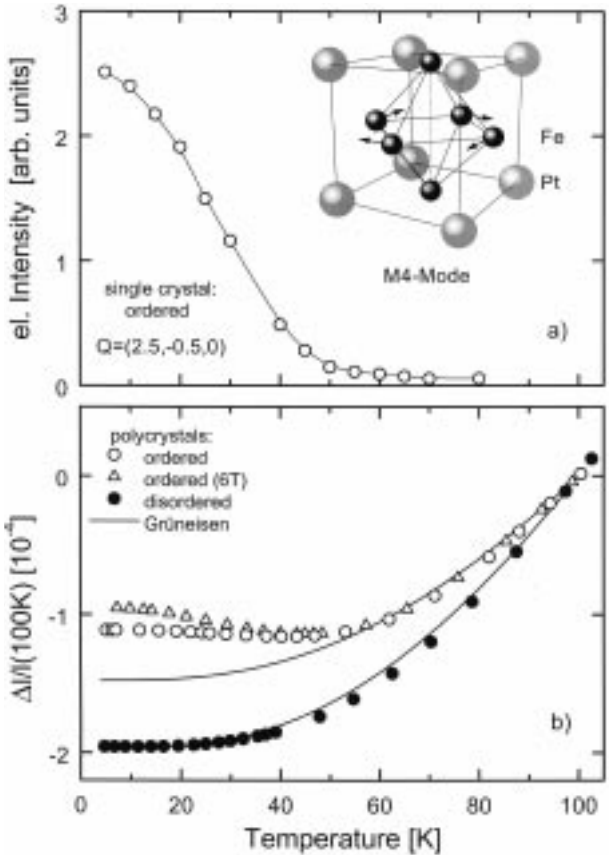

Fig. 6. (a) Intensity of elastic reflection at $Q = (2.5, -0.5, 0)$ *vs.* temperature in ordered $Fe_{72}Pt_{28}$ related to rotation of Fe-octahedrons (M_4-mode) shown in the lattice model. (b) Thermal expansion $\Delta l/l$ *vs.* temperature of polycrystalline $Fe_{72}Pt_{28}$ [30], ($\circ, \bullet$) ordered and disordered, respectively. ($\triangle$) ordered sample after temporal application of magnetic field $B = 6$ T at 4.2 K. Full curves are Grüneisen fits to the data.

in ordered Fe_3Pt [21]. They show that a renormalization of the $TA_1[\xi\xi 0]$-phonon energies in the FM alloy is considerable in the low q-range, which may explain the experimental findings for ordered as well as disordered $Fe_{72}Pt_{28}$. Particular strong softening is, however, found at the zone boundary for the M_4-mode. A condensation of this mode at low temperatures results in an antiferrodistortive phase transition — resembling that of $SrTiO_3$ — from the cubic into a tetragonal lattice where the new unit cell (001) base plane is doubled with respect to the cubic cell and rotated by 45 degrees.

For a discussion of this phase transition and the nature of the low temperature phase, we have replotted in Figure 6b some thermal expansion data previously obtained on polycrystalline ordered and disordered $Fe_{72}Pt_{28}$ below 100 K [30]. As can be seen in this figure, the low temperature thermal expansion of disordered $Fe_{72}Pt_{28}$ can be rather well fitted using a Grüneisen relation $\Delta l/l \propto U(T)$, where U is the thermal energy of the sample, determined from specific heat (see below). For ordered $Fe_{72}Pt_{28}$, this is possible only above about 50 K, as shown in the figure by a solid curve. Below this temperature the thermal expansion significantly deviates from a Grüneisen like behaviour quite in parallel with the development of the superstructure peak shown in Figure 6a. Moreover, this deviation, causing an expansion of the crystal with decreasing temperature, is even enhanced after the temporal application of a 6 T magnetic field at 4.2 K. We note further that both the high and low field magnetizations [31,32] of ordered $Fe_{72}Pt_{28}$ are enhanced below ~ 50 K whereas the low field a.c. magnetic susceptibility [33] exhibits a frequency dependent spin glass like anomaly below this temperature.

These experimental findings on ordered $Fe_{72}Pt_{28}$ have been ascribed, so far, to a not specified premartensitic structural transition. In the light of our present results, we elucidate that the observed magnetic and thermal anomalies arise from the low temperature tetragonal phase induced by the soft M_4-mode. Whereas the static magnetization is increased in this phase, most likely by the increase of the Fe-magnetic moment, the dynamical magnetic behaviour is reduced, presumably by local magnetic anisotropy.

Concerning the enhancement of the static magnetization [31,32], the low temperature thermal expansion anomaly, shown in Figure 6b, is considered as due to the spontaneous magnetovolume-expansion. The ratio between the relative changes $\Delta V/V$ of the volume and $\Delta M/M$ of the magnetization at low temperatures is the same as that of the Invar effect in this material. This effect is pronounced at temperatures close below T_C and characterized by the ratio ω_S/M_S, *i.e.* the ratio of the spontaneous magnetovolume expansion ω_S to the spontaneous magnetization M_S at zero Kelvin. Within this view, the low temperature tetragonal lattice is stabilized by volume expansion with the merit of an increased magnetic moment. Consequently, the dynamical fluctuations into the low temperature phase, mediated by the soft M_4-mode, are considered to be strongly coupled to magnetovolume strain, controlled by the magnetization. This may to some extent explain, why the elastic scattering intensity at the M-point — taken as the order parameter of the low temperature phase — increases continuously with decreasing temperature, whereas the respective phonon energies remain finite and any critical fluctuations near the transition temperature are virtually absent (see *e.g.* the specific heat results further below).

To illustrate how magnetovolume strain couples to the $TA_1[\xi\xi 0]$ phonons, especially to the M-point zone boundary mode, we consider the microscopic theory of the Invar effect: Within our current understanding, the Invar effect in the Fe-rich Invar alloys arises from thermally induced charge transfer between d-bands of different symmetry and bonding character crossing the Fermi surface [2,4]. On the decrease of the temperature, both the atomic magnetic moment and volume increase by charge transfer from a spin minority band with E_g symmetry and nonbonding character into a spin majority band with T_{2g} symmetry and antibonding character. The T_{2g} orbitals of the Fe-atoms point along the [110] directions, *i.e.* along the lines connecting the neighbouring Fe-atoms. One may, therefore, intuitively suspect that by a specific reduction

of symmetry in the low temperature phase and simultaneously by the (in second order) increased distance between the neighbouring Fe-atoms due to the rotated Fe-octahedra (see Fig. 6a) the overlap of the T_{2g} orbitals is reduced, favouring both the enhancement of magnetic moment and volume expansion on further charge transfer into these orbitals. Within a more general view, one may consider the origin of the zone boundary phonon softening in ordered $Fe_{72}Pt_{28}$ as due to a "magnetic" Jahn-Teller like band effect: By lowering the crystal symmetry the degeneracy of electronic states is lifted causing a redistribution of states close to the Fermi surface and a reduction of the total electronic energy by the increase of the magnetic polarization.

Concerning the dynamical magnetic behaviour of ordered $Fe_{72}Pt_{28}$ at low temperatures, we derive from our present results the following: Below $\sim$ 50 K, this crystal is likely to consist of different structural domains, in which the Fe-octahedrons, shown in Figure 6, are rotated around one of the three possible (001) axes, eventually in combination with a slight tetragonal distortion $c/a \lesssim 1$ of the cubic lattice. Within those domains, where the axis of rotation coincides with the direction of magnetization, uniaxial magnetic anisotropy may arise. Alternatively, in domains, where the magnetization is directed transverse to the axes of the rotation, local magnetic anisotropy may act on the Fe-moments located at the respective axes of rotation, eventually resulting in a non colinear spin arrangement. Certainly, further experimental investigations are necessary to elucidate the detailed nature of the magnetic and structural ground state in ordered Fe_3Pt. The present and previous results suggest, however, that magnetic heterogeneity in this material is caused by the interdependences of structural and magnetic domains, where spatial distributions can be apparently influenced by the application of a sufficiently strong magnetic field (Fig. 6b).

3.3 Low temperature specific heat

To characterize the low temperature thermal excitatons in $Fe_{72}Pt_{28}$, we have performed additional specific heat measurements on the same $Fe_{72}Pt_{28}$ crystals, investigated by the neutron scattering experiments, using an adiabatic heat pulse method. The results are collected in Figure 7. We first note that no anomaly in C_p is found to indicate the occurence of a second order structural phase transition in ordered $Fe_{72}Pt_{28}$ below 100 K. Analysing the measured C_p-data of both crystals, small contributions $C_{sw} = \delta T^{3/2}$ due to spin wave excitations have been first subtracted from C_p, taking the values $\delta = 0.28$ and 0.32 mJ $K^{-5/2}$ mol^{-1} for the ordered and the disordered crystal, respectively, derived from previous measurements of the spin wave dispersion on these crystals [34]. Then, from the usual plot of C_p/T *vs.* T^2, shown in the insert of Figure 7, the low temperature electron and phonon contributions to C_p, $C_{el} = \gamma T$ and $C_{ph} = \beta T^3$, have been determined resulting in $\gamma = 9.8$ and 9.2 mJ $mol^{-1}K^{-2}$

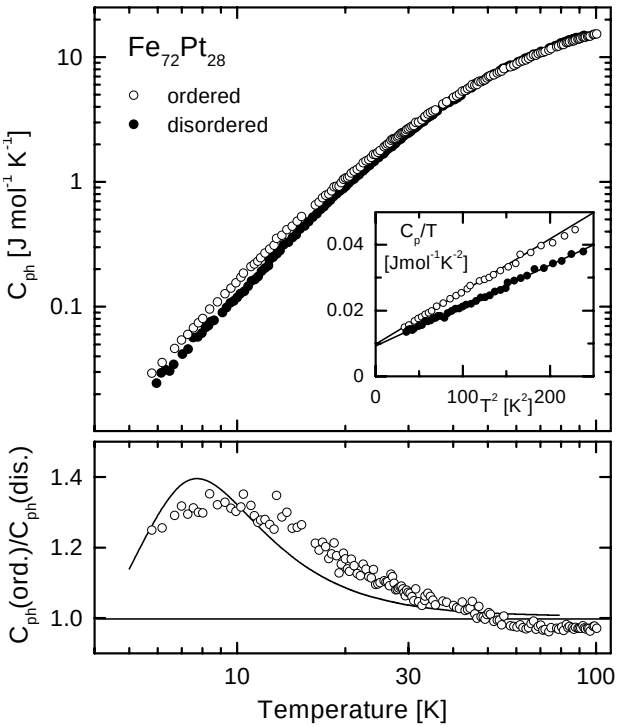

Fig. 7. Lattice contributions C_{ph} to specific heats C_p for ordered and disordered $Fe_{72}Pt_{28}$ (upper panel) and ratio of lattice contributions (lower panel) *vs.* temperature. The inset shows C_p/T *vs.* T^2. Solid curve in lower panel simulates the effect of an Einstein mode $\hbar\omega_E = 3$ meV in the ordered crystal.

for the electronic excitations and in $\beta = 0.157$ and 0.122 mJ $mol^{-1}K^{-4}$, *i.e.* in the low temperature Debye temperatures $\Theta_D = 231$ K and 251 K for the phonon excitations of the ordered and disordered crystal, respectively. Whereas the low temperature electronic contributions to C_p of both crystals do not differ much, the phonon contribution to C_p of the ordered crystal is clearly enhanced above that of the disordered one.

The upper panel of Figure 7 shows the phonon contributions to C_p of both crystals on a double log scale. In the lower panel, the ratio of the two phonon contributions *vs.* $\log T$ is shown. We suggest that the enhancement of C_{ph} in the ordered crystal at low temperatures arises from the enhancement of the low energy phonon density of states due to the soft M-mode. Surprisingly, the temperature where the enhancement becomes obvious, *i.e.* about 50 K, coincides with the start temperature of the central peak development, shown in Figure 6. Taking this, however, merely as fortuitous, we note that above about 50 K the ratio of the phonon specific heats falls to values close below 1. Apparently, for a more detailed comparison of the specific heats of both crystals at higher temperatures, the differences in the phonon densities of states originating from other parts of the Brillouin zone have also to be taken into account. Below about 50 K, however, *i.e.* below a mean thermal energy of 4 meV, the soft M-mode in ordered $Fe_{72}Pt_{28}$ seems to have significant influence on the thermally excited phonon spectrum. To account

for this in the simpliest theoretical model, we have added to the phonon specific heat of the disordered crystal an Einstein term with the mode energy $\hbar\omega_E = 3$ meV, which is close to the measured soft mode energy $\hbar\omega_0 \approx 2.3$ meV of the ordered crystal at low temperatures. The enhancement in C_{ph} resulting from such term of proper weight is shown in the lower panel of Figure 7 as solid curve. With respect to this simple approach, the curve well reproduces the essential difference of the phonon specific heats of both crystals.

4 Summary and conclusions

We have investigated the influence of atomic order on the $TA_1[\xi\xi 0]$ phonon softening in Fe_3Pt Invar by detailed comparison of the wave vector and temperature dependent phonon softening in two $Fe_{72}Pt_{28}$ crystals, one well ordered in the $L1_2$ (Cu_3Au) structure, the other disordered fcc. In the disordered crystal, $TA_1[\xi\xi 0]$ phonon softening occurs within the inner region of the Brillouin zone leading to enhancement of long wave tetragonal strain, quite similar as in fcc Fe-Ni and Fe-Pd Invar. In the ordered crystal, the phonon softening is particular strong at the zone boundary M-point leading to a corresponding antiferrodistortive phase transition into a new low temperature phase.

Comparison of the present results with previously observed magnetic and thermal anomalies in ordered $Fe_{72}Pt_{28}$ reveals that the low temperature phase favours both the enhancement of magnetic polarization and atomic volume, consistent with the current microscopic understanding of the Invar effect in this material. In addition, we have found that magnetic anisotropy likely arises in the low temperature phase of ordered $Fe_{72}Pt_{28}$ due to local magnetic anisotropy within the domains of the different structural variants. More detailed investigations on the magnetic and atomic structure of the low temperature phase in ordered $Fe_{72}Pt_{28}$ would be valuable to elucidate the mutual interactions. Comparison of the present low temperature specific heat results of the two $Fe_{72}Pt_{28}$ crystals reveals characteristic differences of the low energy thermal excitations of the lattice, which can be mainly accounted for by enlargement of the low energy phonon density of states in ordered $Fe_{72}Pt_{28}$ due to the soft M-mode.

We thank P. Stauche for the preparation of the crystals. The kind hospitality during the sabbatical stay of one of the authors (W.P.) at Brookhaven laboratory is gratefully acknowledged. Submission of preliminary theoretical results on the phonon softening in Fe_3Pt and valuable discussions with C. Holtfort are acknowledged as well. Part of this work was supported by Deutsche Forschungsgemeinschaft, SFB 166.

References

1. For a review see: E.F. Wassermann, in *Ferromagnetic Materials*, edited by K.H. Buschow, E.P. Wohlfarth (North Holland, Amsterdam, 1990), Vol. VI.
2. P. Entel, E. Hoffmann, P. Mohn, K. Schwarz, V.L. Moruzzi, Phys. Rev. B **47**, 8706 (1993).
3. E. Hoffmann, H. Herper, P. Entel, S.G. Mishra, P. Mohn, K. Schwarz, Phys. Rev. B **47**, 5589 (1993).
4. E.F. Wassermann, in *The Invar Effect: A sentennial symposium*, edited by J. Wittenauer, Cincinnati (The TMS Society, Philadelphia, 1997), p. 51.
5. E.F. Wassermann, M. Acet, P. Entel, W. Pepperhoff, J. Mag. Soc. Jap. **23**, 385 (1999).
6. M. Acet, E.F. Wassermann, K. Andersen, A. Murani, O. Schärpf, Europhys. Lett. **40**, 93 (1997).
7. M. Schröter, H. Ebert, H. Akai, P. Entel, E. Hoffmann, G.G. Reddy, Phys. Rev. B **52**, 188 (1995-I).
8. For reviews see: S.M. Shapiro, Mat. Sci. Forum **56-58**, 33 (1990); W. Petry, J. Phys. IV France **5**, C2-15 (1995).
9. G. Hausch, J. Phys. F: Metal Phys. **6**, 1015 (1976).
10. K. Tajima, Y. Endoh, Y. Ishikawa, W.G. Stirling, Phys. Rev. Lett. **37**, 519 (1976).
11. Y. Endoh, Y. Noda, Y. Ishikawa, Solid State Commun. **23**, 951 (1977).
12. M. Sato, B. Grier, S.M. Shapiro, H. Miyajima, J. Phys. F **12**, 2117 (1982).
13. K. Sumiyama, M. Shiga, Y. Nakamura, J. Phys. Soc. Jap. **40**, 996 (1976).
14. K. Sumiyama, M. Shiga, M. Morioka, Y. Nakamura, J. Phys. F **9**, 1665 (1979).
15. M. Umemoto, C.M. Wayman, Met. Trans. A **9**, 891 (1978).
16. Y. Noda, Y. Endoh, J. Phys. Soc. Jap. **57**, 4225 (1988).
17. H.C. Ling, W.S. Owen, Acta Metall. **31**, 1343 (1983).
18. H. Seto, Y. Noda, Y. Yamada, J. Phys. Soc. Jap. **59**, 978 (1990).
19. J. Zarestky, C. Stassis, Phys. Rev. B **35**, 4500 (1987).
20. H.C. Herper, E. Hoffmann, P. Entel, W. Weber, J. Phys. IV France **5**, C8-293 (1995).
21. C. Holtfort (private communication).
22. J.A. Krumhansl, J. Phys. IV France **5**, C2-3 (1995).
23. M. Matsui, T. Shimizu, H. Yamada, K. Adachi, J. Phys. Soc. Jap. **48**, 2161 (1980).
24. M. Matsui, K. Adachi, H. Asano, Sci. Rep. RITU A **29**, Suppl. 1, 61 (1981).
25. H. Seto, Y. Noda, Y. Yamada, J. Phys. Soc. Jap. **59**, 965 (1990).
26. S. Muto, R. Oshima, F.E. Fujita, Met. Trans. A **19**, 2723 (1988).
27. W. S. Owen, Mater. Sci. Eng. A **127**, 197 (1990).
28. U. Kawald, P. Schulenburg, H. Bach, J. Pelzl, G. Eckold, G.A. Saunders, J. Appl. Phys. **70**, 1 (1991).
29. K. Sumiyama, Y. Emoto, M. Shiga, Y. Nakamura, J. Phys. Soc. Jap. **50**, 3296 (1981).
30. W. Stamm, thesis, Gerhard-Mercator-Universität Duisburg, 1988.
31. H. Maruyama, J. Phys. Soc. Jap. **55**, 2834 (1986).
32. U. Kirschbaum, thesis, Gerhard-Mercator-Universität Duisburg, 1996.
33. N. Schubert, thesis, Gerhard-Mercator-Universität Duisburg, 1994.
34. N. Rosov, J.W. Lynn, J. Kästner, E.F. Wassermann, T. Chattopadhyay, H. Bach, J. Appl. Phys. **75**, 6072 (1994).